VIP ***The following Communications have been judged by at least two referees to be "very important papers" and will be published online at www.angewandte.org soon:***

Author Profile

"My favorite piece of music is "The Four Seasons" (Antonio Vivaldi).
My biggest motivation is the joy of doing research with my colleagues and students …"
This and more about Kiyotomi Kaneda can be found on page 4778.

News

A. P. Alivisatos

C. M. Lieber

R. G. Cooks

H.-C. zur Loye

Obituaries

Books

Highlights

Atom Tunneling

There and gone: Atoms, such as hydrogen or deuterium, commonly disappear and reappear at different locations in molecular structures. For example, carboxylic acids and hydroxycarbenes isomerize through atom tunneling events. It could happen in your reaction!

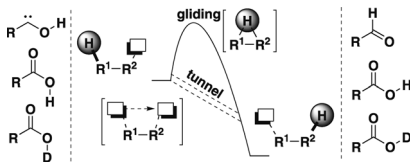

Switching in Vivo

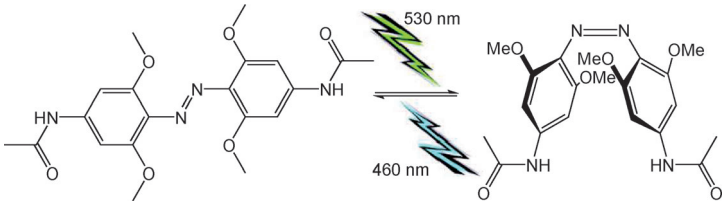

Two bands make light work: Since the isomerization of azobenzenes is usually induced by UV light, its application is limited in living systems. A new azobenzene switch now operates entirely in the visible range. The new design is based on the introduction of OMe groups in the *ortho* positions, which splits the n–π* transition into two absorption bands. The two isomeric forms can be obtained with more than 80% enrichment from the respective photostationary state.

Reaction Monitoring

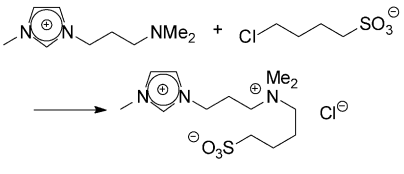

In the swim: Until now, X-ray photoelectron spectroscopy (XPS) has been predominantly applied to the investigation of near-surface regions. Recent work has now brought XPS into a new domain with the direct monitoring of bulk reactions in the liquid phase. In the monitored reaction, the cation of an ionic liquid (IL) reacts with the anion of another IL (see scheme).

For the USA and Canada:
ANGEWANDTE CHEMIE International Edition (ISSN 1433-7851) is published weekly by Wiley-VCH, PO Box 191161, 69451 Weinheim, Germany. Air freight and mailing in the USA by Publications Expediting Inc., 200 Meacham Ave., Elmont, NY 11003. Periodicals postage paid at Jamaica, NY 11431. US POSTMASTER: send address changes to *Angewandte Chemie*, Journal Customer Services, John Wiley & Sons Inc., 350 Main St., Malden, MA 02148-5020. Annual subscription price for institutions: US$ 11.738/10.206 (valid for print and electronic / print or electronic delivery); for individuals who are personal members of a national chemical society prices are available on request. Postage and handling charges included. All prices are subject to local VAT/sales tax.

Minireviews

That's about the size of it: A comparison of structural and magnetic properties of iron oxo based molecular nanomagnets (see picture, right) and magnetic nanoparticles (left) gives a deeper understanding of the magnetic behavior at the intermediate scale between molecular and bulk objects.

Reviews

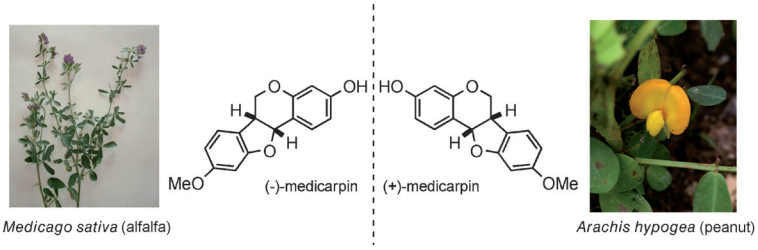

Two sides to the story: The formation of enantiomerically opposite natural products by nature is known, although rare (see examples). To date, many puzzles and stereochemical anomalies remain regarding the biogenesis of these unique natural products, despite the substantial body of research that has been carried out over the years in an attempt to understand the biogenesis of enantiomeric metabolites.

Communications

Traffic cam: A tandem dye prepared from a FRET acceptor and a fluorogenic donor functions as a cell surface ratiometric pH indicator, which upon internalization serves to follow protein trafficking during endocytosis. This sensor was used to analyze agonist-dependent internalization of β_2-adrenergic receptors (see scheme). It was also used as a surrogate antigen to reveal direct surface-to-endosome antigen transfer between dendritic cells (not shown).

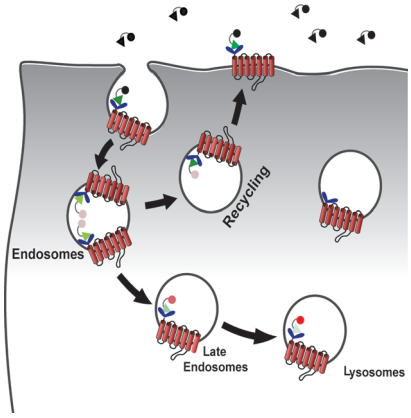

Contact Electrification

In touch: The outcome of contact electrification between dielectrics depends not only on the transfer of charge but also on the transfer of material (see picture). Although only minute quantities of materials are being exchanged during contact, they can reverse the polarity of dielectrics. The reported results corroborate the mosaic model and suggest that the observations are because of the mechanical softness/hardness of the materials.

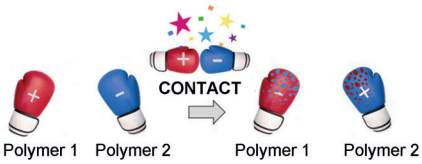

High-Pressure Chemistry

High-pressure ion exchange of small-pore zeolite K-natrolite allows immobilization of nominally non-exchangeable aliovalent cations such as trivalent europium. A sample exchanged at 3.0(1) GPa and 250 °C contains about 4.7 Eu^{III} ions per unit cell, which is equivalent to over 90% of the K^+ cations being exchanged (see picture).

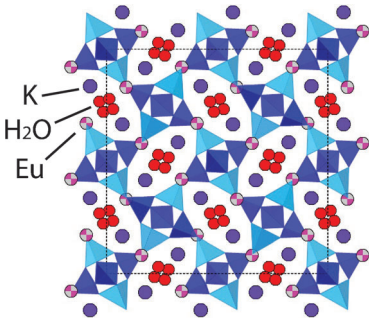

Arresting Particle Growth

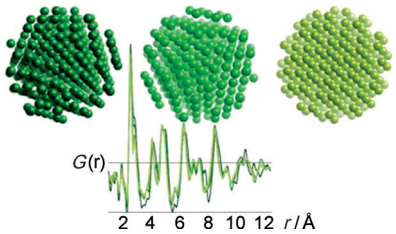

Not simply small particles: Pair distribution function analysis (see picture) yields comprehensive insights into the electrochemical reaction of α-Fe_2O_3 with lithium. The metallic Fe formed in this reaction was found to be defect-rich nanoparticles that restructure continuously without growing—an unusual characteristic likely linked to its highly reversible capacity.

Graphene

An undercover agent: Graphene has been used as an imaging agent to visualize interfacial reactions under its cover, and exhibits a strong confinement effect on the chemistry of molecules underneath (see picture). In a CO atmosphere, CO penetrates into the graphene/Pt(111) interface and reacts with O_2 therein, whereas intercalated CO desorbs from the Pt surface.

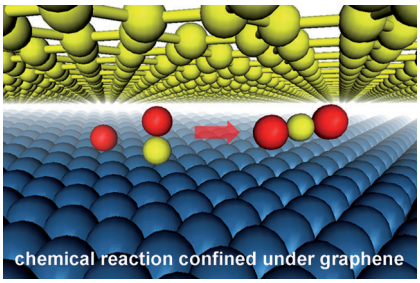

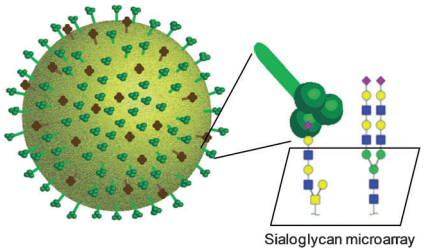

Human influenza viruses are proposed to recognize sialic acids (pink diamonds) on glycans extended with poly-LacNAc chains (LacNAc = (yellow circle + blue square)). N- and O-linked glycans were extended with different poly-LacNAc chains with α2-3- and α2-6-linked sialic acids recognized by human and avian influenza viruses, respectively. The specificity of recombinant hemagglutinins (receptors in green) was investigated by using glycan microarray technology.

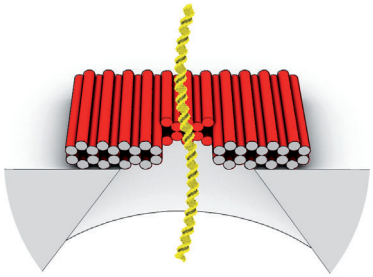

DNA has it covered: DNA origami gatekeeper nanoplates convert nanopores in solid-state membranes into versatile devices for label-free macromolecular sensing applications. The custom apertures in the nanoplates can be chemically addressed for sequence-specific detection of DNA.

In living color: Efficient intracellular covalent labeling of proteins with a photoswitchable dye using the HaloTag for dSTORM super-resolution imaging in live cells is described. The dynamics of cellular nanostructures at the plasma membrane were monitored with a time resolution of a few seconds. In combination with dual-color FPALM imaging, submicroscopic receptor organization within the context of the membrane skeleton was resolved (see figure).

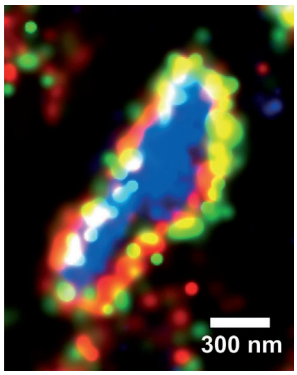

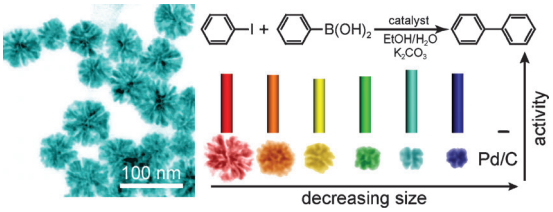

Palladium's pore cousin: A facile approach is described for the size-controlled preparation of porous single-crystalline Pd nanoparticles. These porous Pd nanoparticles exhibit size-independent catalytic activities for the Suzuki coupling and are more active than commercial Pd/C catalysts.

Electron Transfer

Game-SET-match: Pyrrole aminoimidazole alkaloids (PAIs) are metabiosynthesized from chlorinated analogues of oroidin by cell-free enzyme preparations from PAI-producing sponges. Evidence and implications for the biosynthesis of PAIs include putative single-electron transfers (SETs) that promote C—C bond-forming reactions of precursors.

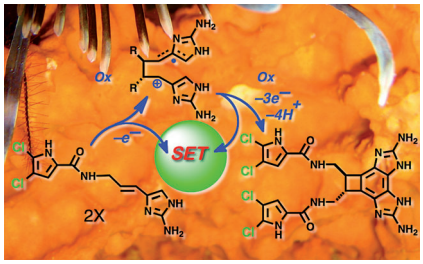

Supramolecular Polymers

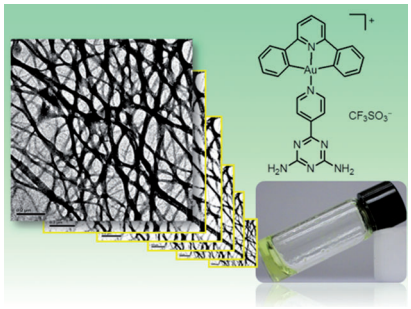

Gold cures: The depicted gold(III) complex self-assembles into supramolecular polymers which form nanofibrillar networks that display sustained cytotoxicity and can also act as carriers for other cytotoxic agents.

Metal–Organic Frameworks

Functionalized linkers can greatly increase the activity of metal–organic framework (MOF) catalysts with coordinatively unsaturated sites. A clear linear free-energy relationship (LFER) was found between Hammett σ_m values of the linker substituents X and the rate k_X of a carbonyl-ene reaction. This is the first LFER ever observed for MOF catalysts. A 56-fold increase in rate was found when the substituent is a nitro group (see picture).

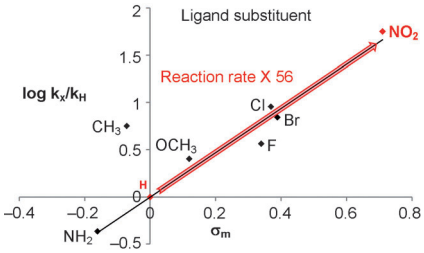

Stem Cell Differentiation

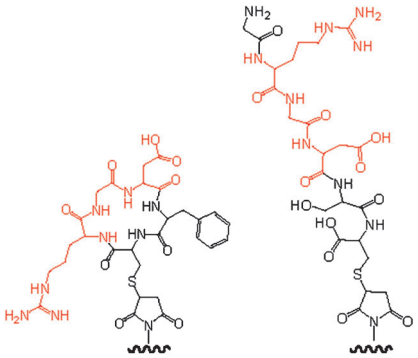

Sticky situation: The differentiation of mesenchymal stem cells can be influenced by the affinity and density of an immobilized ligand for the integrin receptors. Cells adherent to monolayers that present the high-affinity, cyclic-RGD peptide (left) show increased expression of osteogenic markers, while cells on monolayers presenting the lower-affinity, linear-RGD peptide (right) express early markers of myogenesis at a high density and neurogenesis at a low density of the ligand.

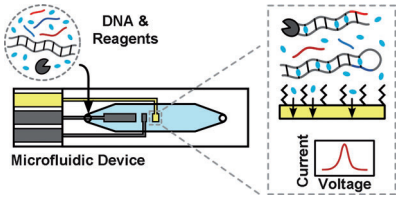

Single-step DNA detection: A microfluidic electrochemical loop mediated isothermal amplification platform is reported for rapid, sensitive, and quantitative detection of pathogen genomic DNA at the point of care (see picture). DNA amplification was electrochemically monitored in real time within a monolithic microfluidic device, thus enabling the detection of as few as 16 copies of *Salmonella* genomic DNA through a single-step process in less than an hour.

Point-of-Care Diagnostics

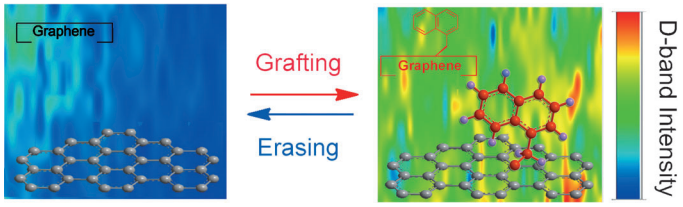

The Kolbe electrochemical oxidation strategy has been utilized to achieve an efficient quasireversible electrochemical grafting of the α-naphthylmethyl functional group to graphene. The method facilitates reversible bandgap engineering in graphene and preparation of electrochemically erasable organic dielectric films. The picture shows Raman D-band maps of both systems.

Graphene

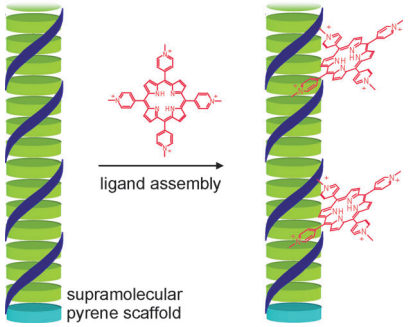

Getting organized: DNA-like supramolecular polymers formed of short oligopyrenotides serve as a helical scaffold for the molecular assembly of ligands (see picture). The cationic porphyrin meso-tetrakis(1-methylpyridin-4-yl)porphyrin interacts with the helical polymers in a similar way as with poly(dA:dT).

Nanotemplates

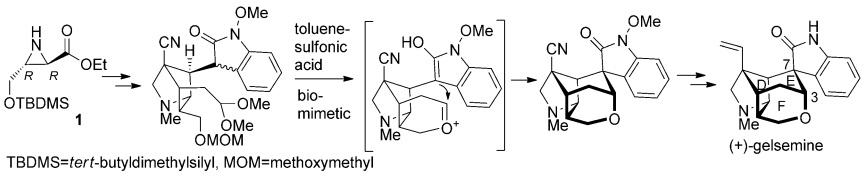

Challenging: (+)-gelsemine was synthesized from (*R*,*R*)-aziridine **1** in 25 steps with approximately 1% overall yield. A multistep, one-pot enol–oxonium cyclization cascade was used to construct, simultaneously, the E ring, F ring, C3 stereocenter, and C7 quaternary stereocenter. This synthesis using the enol–oxonium cyclization reaction as a key step to make the cage structure has demonstrated the proposed biosynthetic pathway of the gelsemine family.

Natural Products

Flexible Pores

Crystallographic pressure-lapse snapshots of a porous material responding to gas loading were used to investigate the stepwise uptake of carbon dioxide and acetylene molecules into discrete confined spaces. Based on the data, a qualitative statistical mechanical model was devised that reproduces even subtle features in the experimental gas sorption isotherms.

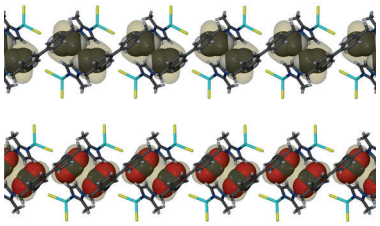

Transmetalation

It's the second step that counts: Arylation of Pd by Au takes place through transition states and intermediates featuring strong Au···Pd metallophilic interactions (see picture). However, the aryl transfer from [AuArL] to [PdArClL$_2$] is thermodynamically disfavored and will not occur unless an irreversible Ar–Ar coupling from [PdAr$_2$L$_2$] follows.

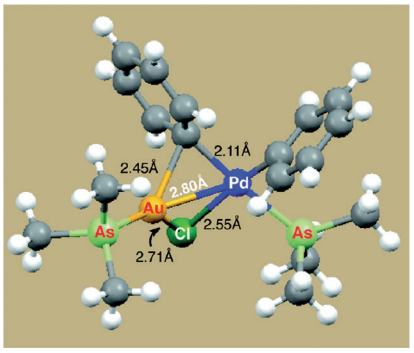

Phosphaorganic Chemistry

Light without fright: A synthetic route to fluorescent primary phosphanes (RPH$_2$) that are resistant to air oxidation both in the solid state and in chloroform solution is described. These versatile precursors undergo hydrophosphination to give tripodal ligands and subsequently fluorescent transition-metal complexes.

Infrared Spectroscopy

The fundamentals: The IR spectrum of the adamantane cation, $C_{10}H_{16}^+$, has been derived by resonant IR photodissociation of weakly bound $C_{10}H_{16}^+ \cdot L_n$ clusters (see picture). The analysis of the IR spectrum provides the first spectroscopic characterization of this fundamental cycloalkane carbocation in the gas phase and direct evidence for the Jahn–Teller distortion in the $^2A_1$ ground electronic state.

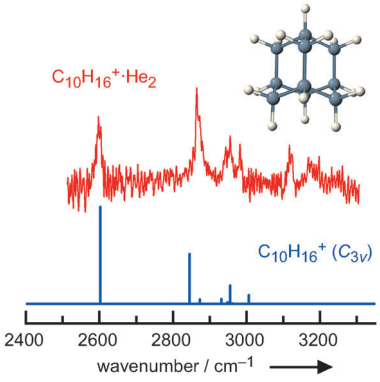

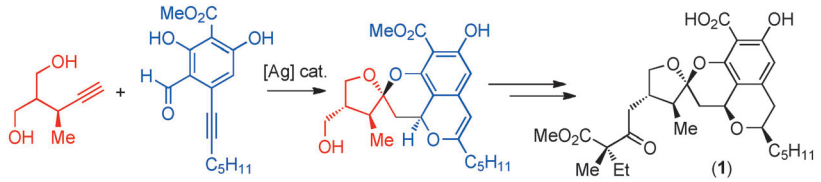

Supply chain: The polycyclic core of (−)-berkelic acid (**1**) was constructed in just one step from very simple starting materials. The total synthesis of **1** involves a seven-step linear sequence. Protection/deprotection steps were avoided and all but the last step were performed on a gram scale. This synthesis could solve the supply problem associated with the exhaustion of the natural source.

Natural Products

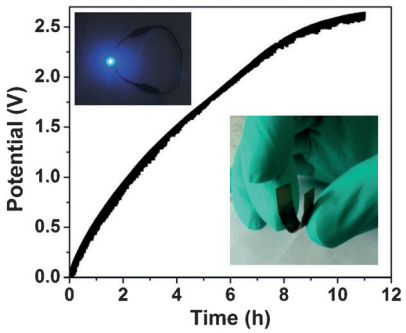

Energy storage on paper: Paper-based, all-solid-state, and flexible supercapacitors were fabricated, which can be charged by a piezoelectric generator or solar cells and then discharged to power a strain sensor or a blue-light-emitting diode, demonstrating its efficient energy management in self-powered nanosystems (see picture).

Self-Powered Nanosystems

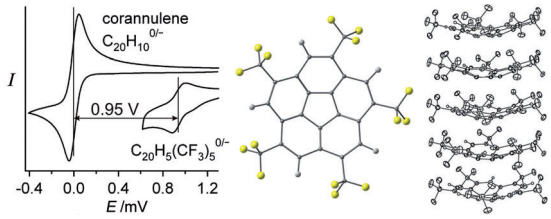

Lots of potential: A trifluoromethylated corannulene, C_5-$C_{20}H_5(CF_3)_5$, has been prepared and characterized spectroscopically and by X-ray crystallography. The structure exhibits a highly ordered bowl stacking that is unusual for corannulenes with acyclic substituents. The first reduction of C_5-$C_{20}H_5(CF_3)_5$ is anodically shifted by 0.95 V, making it the strongest corannulene-based electron acceptor to date.

Corannulenes

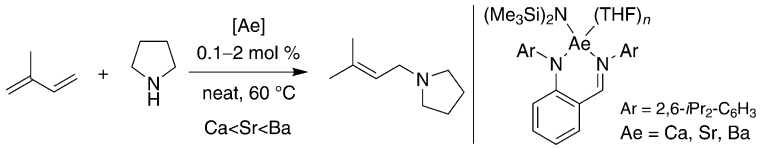

New alkaline-earth amido complexes catalyze the regioselective intermolecular hydroamination (see scheme; Ae = alkaline earth) and hydrophosphination of styrene and isoprene with unprecedented activities. The catalytic performances increased linearly with the size of the metal.

Synthetic Methods

Aromatic Cations

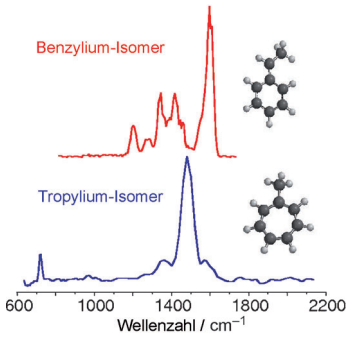

Definitely different: The path towards sorting out a long-standing dichotomy in carbocation chemistry is disclosed by infrared multiple photon dissociation spectroscopy of tropylium and benzylium isomers of $C_8H_9^+$ ions (see picture).

C–H Activation

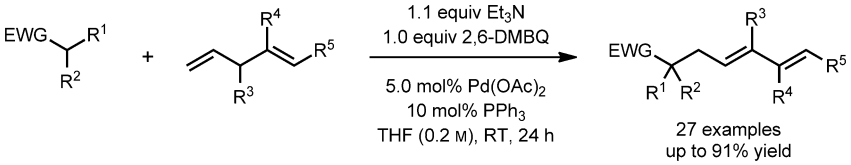

Activated: The title reaction proceeds with a broad range of nucleophiles and variously substituted 1,4-dienes under mild conditions, and provides direct access to the corresponding 1,3-diene-containing products with high regio- and stereocontrol (see scheme; 2,6-DMBQ = 2,6-dimethylbenzoquinone, EWG = electron-withdrawing group). This is the first catalytic allylic C–H alkylation that proceeds in the absence of sulfoxide ligands.

Surface Chemistry

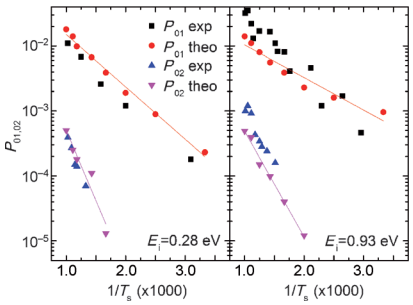

Surface phenomena: Measurements of absolute probabilities are reported for the vibrational excitation of NO(v=0→1,2) molecules scattered from a Au(111) surface. These measurements were quantitatively compared to calculations based on ab initio theoretical approaches to electronically nonadiabatic molecule–surface interactions. Good agreement was found between theory and experiment (see picture; T_s = surface temperature, P = excitation probability, and E = incidence energy of translation).

Organocatalysis

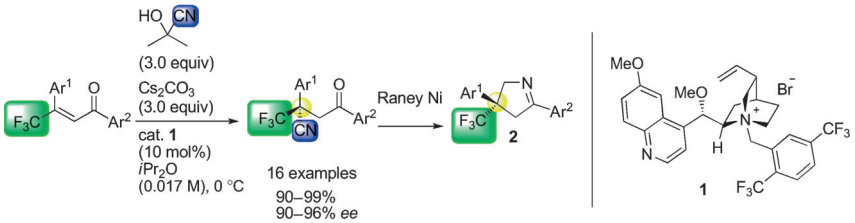

Ether way: The cinchona-alkaloid-catalyzed title reaction was achieved in high yields with high to excellent *ee* values for the first time, and affords key intermediates for the biologically important **2** having a trifluoromethylated all-carbon quaternary chiral center. Ether-type catalysts (**1**) are more efficient in this transformation than the conventional hydroxy analogues.

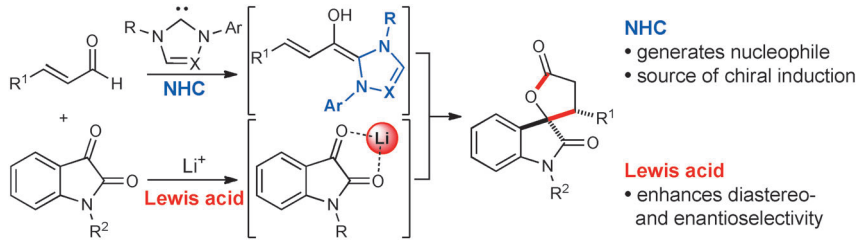

A cooperative catalysis approach for the enantioselective formal [3+2] addition of α,β-unsaturated aldehydes to isatins has been developed. Homoenolate annulations of β-aryl enals catalyzed by an N-heterocyclic carbene (NHC) require the addition of lithium chloride for high levels of enantioselectivity. This NHC-catalyzed annulation has been used for the total synthesis of maremycin B.

Asymmetric Catalysis

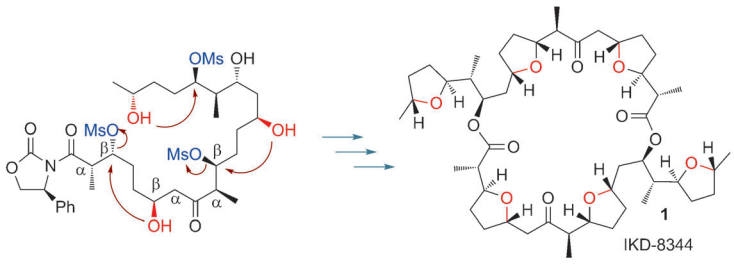

A highly efficient enantioselective total synthesis of the natural antibiotic IKD-8344 is achieved through a convergent route. This route features an otherwise impossible concurrent formation of the THF rings from a linear polyketide precursor through intramolecular O alkylations of mesylates in competition with normally rather facile β elimination and/or α racemization reactions (see scheme, Ms = methanesulfonyl).

Natural Product Synthesis

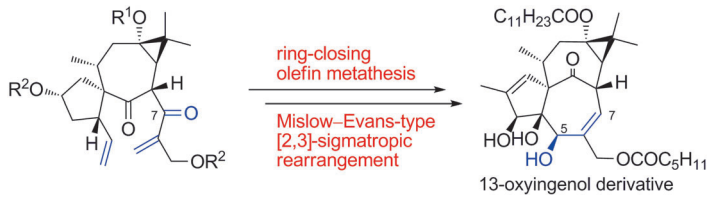

Ring functionalization: The total synthesis of a natural derivative of (−)-13-oxyingenol, a potent anti-HIV diterpenoid, is reported. The key steps in this synthesis include a ring-closing olefin metathesis and a Mislow–Evans-type [2,3]-sigmatropic rearrangement. This synthesis provides access to (−)-13-oxyingenol and its natural derivative in 21 steps from a synthetic intermediate previously prepared by Kigoshi and co-workers.

Natural Product Synthesis

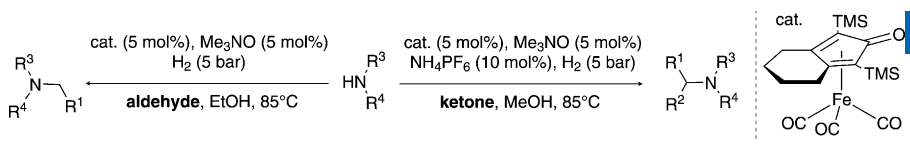

An aminated series: A well-defined iron-catalyzed reductive amination reaction of aldehydes and ketones with aliphatic amines using molecular hydrogen is presented. Under mild conditions, good yields for a broad range of alkyl ketones as well as aldehydes were achieved.

Reductive Amination

Synthetic Methods

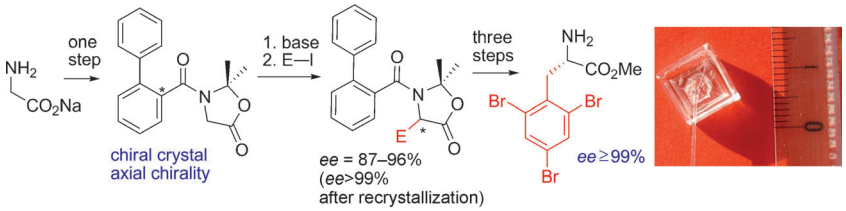

Frozen: The spontaneous crystallization of an achiral compound in a chiral conformation is used as the unique source of chirality in an absolute asymmetric synthesis of tertiary amino acids. The dynamic axial chirality of tertiary aromatic amides is frozen in a crystal (see picture) and is responsible for the stereoselectivity of the deprotonation/alkylation (see scheme). α-Amino acid derivatives are synthesized in up to 96% *ee*.

Coordination Chemistry

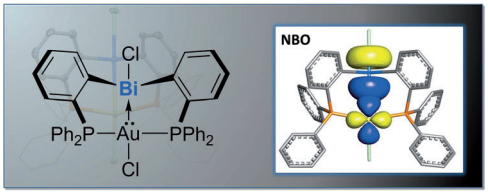

BiZness as usual? Not exactly! The bismuth atom of the tridentate diphosphinobismuthine (*o*-$(Ph_2P)C_6H_4)_2BiCl$ behaves as a Z rather than L ligand when in the coordination sphere of late transition metals such as gold. The σ-acceptor behavior of Bi is supported by its disphenoid coordination geometry and theoretical studies, which show a Au→Bi interaction.

Metallophilic Interactions

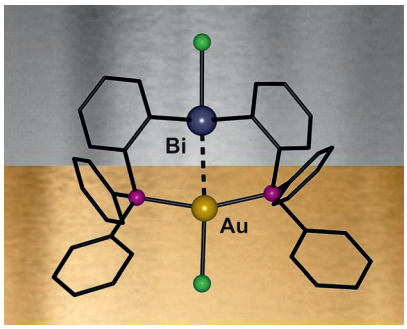

Noble metals meet a heavyweight: A pincer ligand brings together bismuth with gold and platinum, so that metallophilic interactions are established. According to DFT calculations, these interactions contain dominant metal→bismuth contributions.

Crystallization Processes

Setting cement: Highly dynamic hydration processes that occur during the first seconds of cement hydration were studied by time-resolved synchrotron X-ray diffraction. Polycarboxylate ether additives were found to influence the formation of the initial crystalline hydration products on a molecular level.

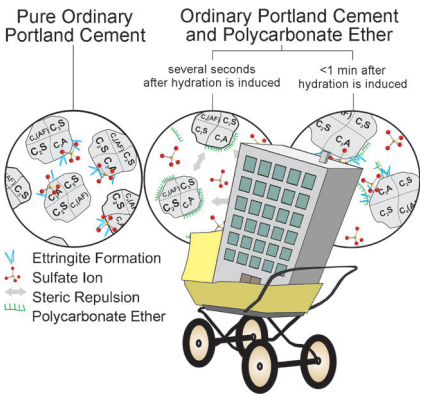

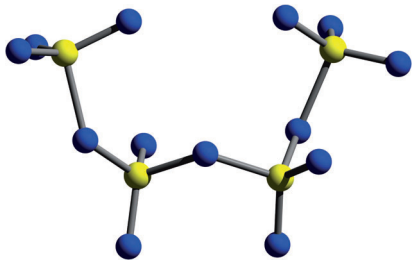

Sulfates united: The unique tetrasulfate $S_4O_{13}^{2-}$ anion was observed in the structure of $(NO_2)_2[S_4O_{13}]$ that forms in the reaction of N_2O_5 with SO_3. Theoretical investigations show that the anion is a stable member of the polysulfate series $[S_nO_{3n+1}]^{2-}$, which was investigated up to $n=11$.

Polysulfates

Shine a light: A circular dichroism effect in the ±10% regime on randomly oriented chiral molecules in the gas phase is demonstrated. The signal is derived from images of photoelectron angular distributions (see picture) produced by resonance-enhanced multiphoton ionization and allows the enantiomers to be distinguished. To date, this effect could only be generated with a synchrotron source. The new tabletop laser-based approach will make this approach far more accessible.

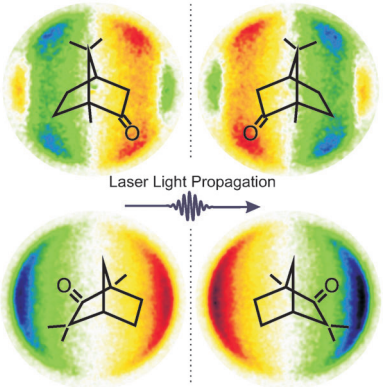

Chirality

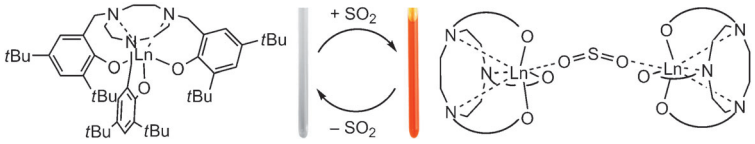

Easy come, easy go: The first molecular SO_2 complexes of the lanthanides (Ln = Sm, Eu) have been prepared. The compounds can reversibly coordinate gaseous SO_2. Concomitant with the addition and removal of SO_2, the color of the complexes changes reversibly (see scheme). The structures of the SO_2 compounds could be confirmed in solution and in the solid state.

Reversible SO_2 Coordination

Supporting information is available on www.angewandte.org (see article for access details).

A video clip is available as Supporting Information on www.angewandte.org (see article for access details).

This article is available online free of charge (Open Access).

This article is accompanied by a cover picture (front or back cover, and inside or outside).

Service